Improvements of Lagrangian Data Assimilation Tested in the Gulf of Mexico

JUNJIE DONG,[a] LUYU SUN,[a] JAMES A. CARTON,[a] AND STEPHEN G. PENNY[b,c]

[a] *Department of Atmospheric and Oceanic Science, University of Maryland, College Park, College Park, Maryland*
[b] *Sofar Ocean, San Francisco, California*
[c] *Cooperative Institute for Research in Environmental Sciences, University of Colorado Boulder, Boulder, Colorado*

(Manuscript received 29 July 2022, in final form 21 April 2023, accepted 23 April 2023)

ABSTRACT: This study extends initial work by Sun and Penny and Sun et al. to explore the inclusion of path information from surface drifters using an augmented-state Lagrangian data assimilation based on the local ensemble transform Kalman filter (LETKF-LaDA) with vertical localization to improve analysis of the ocean. The region of interest is the Gulf of Mexico during the passage of Hurricane Isaac in the summer of 2012. Results from experiments with a regional ocean model at eddy-permitting and eddy-resolving model resolutions are used to quantify improvements to the analysis of sea surface velocity, sea surface temperature, and sea surface height in a data assimilation system. The data assimilation system assimilates surface drifter positions, as well as vertical profiles of temperature and salinity. Data were used from drifters deployed as a part of the Grand Lagrangian Deployment beginning 20 July 2012. Comparison of experiment results shows that at both eddy-permitting and eddy-resolving horizontal resolutions Lagrangian assimilation of drifter positions significantly improves analysis of the ocean state responding to hurricane conditions. These results, which should be applicable to other tropical oceans such as the Bay of Bengal, open new avenues for estimating ocean initial conditions to improve tropical cyclone forecasting.

KEYWORDS: Currents; Sea level; Sea surface temperature; Tropical cyclones; Data assimilation

1. Introduction

Tropical cyclones (TCs), which are among nature's most destructive phenomena, cause profound changes to the stratification and circulation of the tropical oceans. This study uses of regional ocean model at 1/4° eddy-permitting and 1/12° eddy-resolving model resolutions to test improvements to estimates of those changes through application of a new approach to directly assimilate observed surface drifter paths as those drifters respond to the passage of a TC (known as a hurricane in the Atlantic). The new approach uses an augmented-state Lagrangian data assimilation (LaDA) based on the local ensemble transform Kalman filter (LETKF; Hunt et al. 2007; Sun and Penny 2019; Sun et al. 2022). Our investigation highlights the importance of model resolution for updating sea surface velocity, sea surface temperature (SST), and sea surface height (SSH) under realistic conditions associated with the passage of Hurricane Isaac through the Gulf of Mexico in summer, 2012. To make the experiments as realistic as possible, in addition to the Grand Lagrangian Deployment (GLAD) (Özgökmen 2012) Program surface drifters we also assimilate in situ profile measurements of temperature and salinity. Analysis of the experiment results shows that when the model grid is eddy resolving, assimilating drifter paths can significantly improve the response of the upper ocean to the passage of a TC, both in its impact on surface currents, and on stratification and vertical motion.

The domain we focus on in this study is the semi-enclosed Gulf of Mexico (GoM). The GoM receives 25 Sv (25×10^6 m^3 s^{-1}) of warm tropical water from the southern Caribbean, flowing northward through the Yucatan Channel, where it enters the Loop Current and eventually exits through Florida Straits (Cardona and Bracco 2016). Surface temperatures range from less than 15°C in the coastal zone in winter to over 29°C in the central basin. The high TC heat potential of the GoM water is reflected in the depth of the 26°C isotherm, which extends to 200 m or deeper within and south of the Loop Current. These warm upper-ocean temperatures contribute to the passage of an average of six hurricane-strength storms through the GoM during June–October each year. The path of the Loop Current frequently develops long hairpin extensions northward toward the coast of Louisiana. In such circumstances 200-km diameter anticyclonic eddies can shed from the Loop Current. Observations suggest this shedding occurs at a rate of 1–3 yr^{-1}. These warm core Loop Current eddies are observed to propagate westward at speeds of 2–5 km day^{-1}, eventually dissipating along the east coast of southern Texas or Mexico. Again, because of their contributions to TC heat potential, the path of the Loop Current and the positions of the warm core eddies are high priority analysis targets for GoM hurricane forecasting systems.

Surface drifters are relatively inexpensive floats that include satellite tracking to ascertain position information. They can be drogued at 10–20-m depth to reduce wind effects and achieve better agreement with surface currents and are often fitted with a near-surface thermistor and sometimes a salinity sensor. For example, since the early 1980s the Global Drifter Program has deployed thousands of drogued surface drifters throughout the global ocean (Elipot and Lumpkin 2008; Lumpkin et al. 2017). In this study we focus on the group of around 300 surface drifters deployed by the GLAD in the northern GoM (Özgökmen 2012) in summer 2012. The GLAD array was present when Isaac entered the southeastern GoM

Corresponding author: Luyu Sun, lysun@umd.edu

DOI: 10.1175/MWR-D-22-0202.1

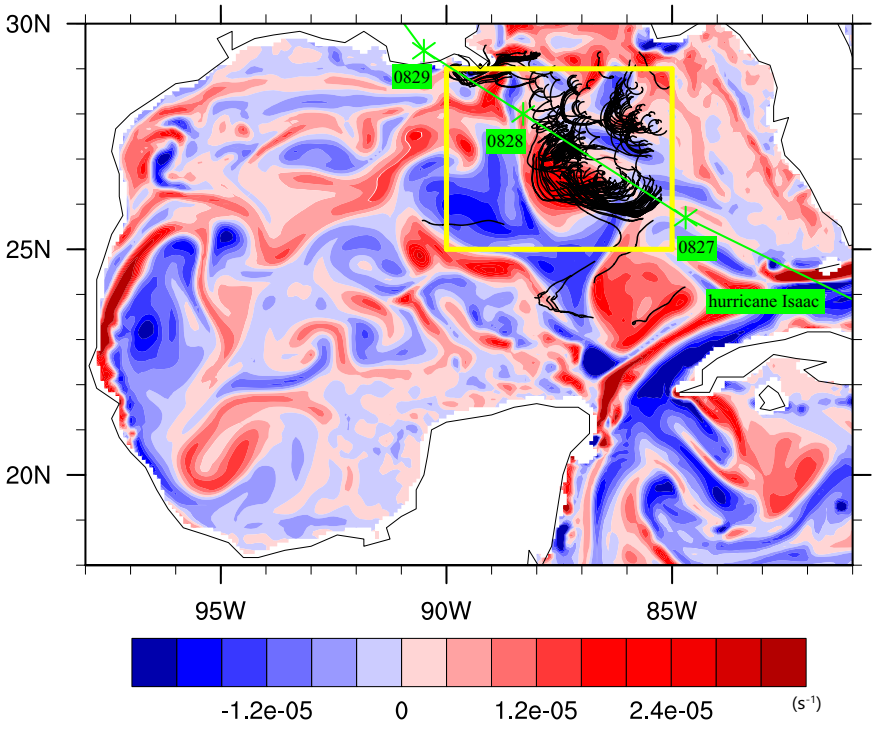

FIG. 1. Plots of 206 GLAD surface drifter trajectories from 27 to 29 Aug 2012 (black lines). The yellow-outlined box highlights the research area. The green line shows the track of Hurricane Isaac. The background shading shows surface vorticity based on the GLORYS12V1 reanalysis data on 28 Aug 2012 (s^{-1}; here and in the Fig. 2 color label "e-05" indicates "$\times 10^{-5}$"). Note that the GLAD surface drifters are mainly located inside the yellow box, and Hurricane Isaac passed through the yellow box on 28 Aug 2012.

early on 27 August with a minimum central pressure of 975 mb (Fig. 1). Isaac slowly strengthened to a category-1 Hurricane (119–153 km h^{-1}) with the minimum central pressure dropping to 965 mb at 0300 UTC 29 August as it traveled north-northwest, tracking along the path of the Loop Current. Isaac gradually weakened after making landfall at 1800 UTC 29 August. The intense near-surface conditions associated with the passage of Isaac caused a number of the GLAD surface drifters to be lost (Muscarella et al. 2015).

The most common way to assimilate surface drifter position data is to convert location differences (e.g., at a daily frequency) into approximate Eulerian velocities and then assimilate those Eulerian velocities using a multivariate optimal interpolation scheme (Molcard et al. 2003; Ishikawa et al. 1996). Extension of this approach to a Kalman filter in a point vortex system was carried out by Kuznetsov et al. (2003) and Ide et al. (2002) who presented a technique for the direct assimilation of Lagrangian data using the augmented tracer advection equations that track the correlation between the flow and the drifter paths. An experiment toward treating the drifter path observations as Lagrangian variables was carried out by Nodet (2006) in an idealized study in the context of variational assimilation, who showed in that scenario that LaDA is more accurate than Eulerian assimilation. Nodet (2006) also found that LaDA reduces the spurious mixing that is introduced when using Eulerian assimilation under conditions where the observation window is longer than a few inertial periods. Taillandier and Griffa (2006) further improved the velocity analysis by introducing constraints on mass conservation and imposing the requirement of geostrophic equilibrium. Nilsson et al. (2012) confirmed the Taillandier and Griffa (2006) result in a realistic study of the circulation of the Mediterranean Sea in the context of a three-dimensional variational assimilation scheme. To restore the inadequate spatial and temporal resolution of geostrophic velocities derived from altimetry data and surface Ekman current velocities derived from forecast winds, Berta et al. (2015) applied another realistic study in the GoM, combining altimetry maps with drifter trajectory data to produce Eulerian velocity fields with a spatial resolution of 10 km and a temporal resolution of 1 h. Vernieres et al. (2011) showed that assimilation of trajectory data constrains the ocean surface field to capture eddy variation in GoM more effectively than the assimilation of transformed Eulerian velocity proxy observations by using synthetic data from a multilayer reduced gravity model control run. Finally, Issa et al. (2016) extended the study of Nilsson et al. (2012) to include more frequent velocity updating, additional improvements to the velocity estimation near the coast, and more accurate estimation of eddy dimension and intensity.

Sun and Penny (2019) proposed an augmented-state LaDA approach using LETKF (hereinafter LETKF-LaDA), which

allows for the assimilation of multiple drifter measurements. In this algorithm, the definition of the localization region remains the same as the original LETKF algorithm for assimilating both conventional in situ profile observations and the Lagrangian observations (Sun and Penny 2019; Sun et al. 2022). The observation operator defined for each localization region is augmented to contain the localized linear observation operator for both the temperature and salinity profiles and the drifter measurements. This modification allows for defining parameters such as the localized observation error covariance matrix and the localized forecast perturbation matrix within the observation space for both of the in situ and drifter states. By implementing the original LETKF in each localized region, the localized analysis can be obtained for all the augmented model states (including gridded ocean states and Lagrangian drifter states).

In a realistic case study of LETKF-LaDA in the GoM during summer of 2012 with GLAD drifters, Sun et al. (2022) explored the impact of vertical localization (where the influence of the drifter information is limited to the upper ocean and does not extend below the thermocline). Assimilation of historical in situ temperature and salinity profiles, surface drifter positions, and derived velocities from the GLAD field experiment was performed. As compared with the Eulerian approach, in synoptic scale, they found that the presence of a sufficient number of drifters improved accuracy of temperature, salinity, and kinetic energy analysis down to 500–600-m depth. In this study, we use the experiments conducted in Sun et al. (2022) and extend the analysis to focus on the application of LETKF-LaDA during the actual passage of Hurricane Isaac, rather than synoptic accuracy improvement during the whole period of the GLAD field campaign. The experiment methodology is discussed in section 2. Results about the surface vorticity field and fine hurricane-induced changes in temperature and salinity at different levels are discussed in section 3.

2. Materials and methods

Our regional model uses the new Geophysical Fluid Dynamics Laboratory Modular Ocean Model, version 6 (MOM6; NOAA-GFDL 2021), numerics in a 2×10^6 km^2 regional domain (18°–30.5°N and 262°–279.5°E) during the 2-month period from 1 August to 29 September 2012. Two horizontal resolutions are considered: 1) an eddy-permitting $1/4° \times 1/4°$ grid and 2) an eddy-resolving $1/12° \times 1/12°$ grid. Each has the same set of 75 vertical z^*-coordinate levels with 2–3-m resolution in the top 50 m. The model has biharmonic Smagorinsky-type nonlinear eddy viscosity. The open boundary conditions set the Laplacian of the flow to zero in this biharmonic viscosity term. Parameterizations are also included for shear-driven and internal tide-driven mixing. No tidal constituents were imposed on the open boundary (the GoM is unusual in having a dominant diurnal lunar tide).

Initial conditions and time-dependent open boundary conditions of temperature, salinity, and velocity are provided by the Simple Ocean Data Assimilation, version 3.4.2, ocean reanalysis (Carton et al. 2018). Instantaneous snapshots of the modeled temperature and salinity fields are output every 6 h, along with the position data for a set of simulated drifters. The ensemble LETKF-LaDA requires separate forcing fields for each ensemble member to reflect the uncertainty in surface forcing. The ensemble of atmospheric forcing fields is provided by the Twentieth Century Reanalysis, version 3 (20CRv3; Slivinski et al. 2019).

The observation dataset includes all quality-controlled temperature and salinity profile observations contained in the World Ocean Database 2018 (Boyer et al. 2018). To evaluate the performance of our experiments, we use the GLORYS12V1 reanalysis (Lellouche et al. 2021) downloaded from the European Copernicus Marine Environment Monitoring Service that has $1/12° \times 1/12° \times 50$ vertical level resolution. The GLORYS12V1 reanalysis is based on the Nucleus for European Modeling of the Ocean (NEMO; Madec and the NEMO Team 2008), driven at surface by 3-hourly atmospheric boundary conditions from ECMWF ERA-Interim reanalysis (Dee et al. 2011). It presents with an average horizontal resolution of 1/12° and 50 depth layers with a resolution ranging from less than 1 m near the surface to 450 m near the bottom. Incorporating a singular evolutionary extended Kalman filter (SEEK) with a three-dimensional variational multivariate background error covariance matrix (Lellouche et al. 2013), it assimilates along-track altimeter sea level anomaly, satellite sea surface temperature, sea ice concentration, and vertical profiles of temperature and salinity in situ. GLORYS12V1 is heavily constrained by its use of observed satellite altimetry, meaning that scales larger than the 100-km radius of deformation are generally well represented. It effectively captures interannual climate variability signals for oceans and sea ice. Quality assessments have shown that, across the in-analysis dataset, the regional error is less than 0.4°C and the global mean sea surface temperature is close to the observed value, with a mean error of less than 0.1°C, as well as representing the small-scale variability of surface dynamics particularly well (Jean-Michel et al. 2021). The dataset has sufficient performance to serve as a reliable reference for the large-scale surface variables and vertical profile fields for this study. This study, however, assimilated not only the same Argo drifter observations as GLORYS12V1, but also about 240 more drifter observations from the GLAD and profiling float (PFL), expendable bathythermographs (XBT), conductivity-temperature–depth measurements from the World Ocean Database. The features of sea surface variables in GLORYS12V1 may be poorly resolved or missing altogether, which will be analyzed later.

We applied the LETKF/LETKF-LaDA algorithms for all the DA experiments with an ensemble size of 30 members (i.e., $K = 30$). The 6-h assimilation windows are used throughout the study period. To achieve localization, an individual analysis is conducted at every grid point, utilizing localized observations within a prescribed region defined by a geospatial radius. A double size of the baroclinic Rossby radius of deformation (Chelton et al. 1998) is initially set as the horizontal localization radius for both the profile and the surface drifter measurements. A cutoff vertical localization to the assimilation of drifter positions was added to this study, which

restricts the influence of surface drifter position observations to remain above the ocean mixed layer (OML), instead of the entire water column. In accordance with Sun et al. (2022), it is found that assimilation of surface drifter positions without vertical localization can cause temperature and salinity estimates to be degraded below the OML. Meanwhile, the assimilation of temperature and salinity profiles is configured to use no vertical localization, which enables profile observations of the ocean to impact the entire water column, thus preserving vertically consistent dynamics and improving results (Sluka et al. 2016; Penny et al. 2015). In general, the OML is shallower than 70 m but can deepen to 150 m in the Loop Current (Trent 2006). In this study, the cutoff OML depth for the vertical localization is determined at each time step by using the modeled ensemble mean OML depth, and the corresponding localization function is

$$f(\Delta h) = \begin{cases} 1, & \text{if } \Delta h < \text{mean OML depth} \\ 0, & \text{if } \Delta h \geq \text{mean OML depth} \end{cases},$$

where Δh is the height difference between the forecast ocean fluid states and the surface drifter observations.

Results are presented from three sets of experiments carried out using the same initial conditions and surface forcing:

1) free model integrations using 1/12° horizontal model resolution (experiments: FREE),
2) in situ temperature and salinity profile observations are assimilated every 6 h into both the 1/4° and 1/12° models (experiments: PROF), and
3) in situ temperature and salinity profile observations, as well as the surface drifter GPS locations, are assimilated every 6 h into the 1/4° and 1/12° models using the augmented-state LaDA (experiments BOTH) with a vertical localization down to the OML depth on drifter measurements as aforementioned.

3. Results

Our presentation of the results focuses on the changing ocean conditions in response to the passage of Hurricane Isaac. We discuss surface velocity, SSH, and hydrography successively as they are represented in the different sets of experiments. Underlying themes are the extent to which we can quantify the impact of introducing the augmented-state LaDA and also the extent to which we can separate the relative contributions of the surface drifters and conventional hydrographic observations.

a. Surface velocity

As Isaac passes through the study focus area on 28 August (Fig. 2) the GLORYS12V1 reanalysis reveals a stationary pair of cyclonic (cold core) and anticyclonic (warm core) eddies, indicated by boxes A and B. The experiment FREE, likewise, shows these stationary eddies but with increased spatial extent and intensity of the cyclonic eddy located near the hurricane center on 28 August (Fig. 2c), and a corresponding increase in its central relative vorticity of 4×10^{-6} s^{-1}. The surface vorticity can be converted to geostrophic estimates of the Laplacian of SSH by multiplying by $f/g \sim 1.3 \times 10^{-5}$ s m^{-1}. Assimilating the temperature and salinity profiles (experiment PROF, Figs. 2f–j) shows that a large area of anticyclonic rotation (negative vorticity) in box B near the center of the hurricane on 28 August becomes cyclonic and, as in experiment FREE, the strength of the vorticity center increases by about 4×10^{-6} s^{-1}. In contrast to the GLORYS12V1 reanalysis, even though the assimilation of hydrographic profiles alone is successful in improving the fine detail of the vorticity field, PROF fails in maintaining the stationary pair of eddies.

When we additionally assimilate drifter positions (experiment BOTH), not only does the vorticity field have fine-scale details but also the position and strength of cyclonic eddies are also more consistent with the GLORYS12V1 reanalysis than experiment PROF. The progression of the response is described in Figs. 2k–o, which show several centers of positive and negative vorticity in box B before Isaac enters the study area; these are mesoscale details that do not appear in other experiments. As Isaac enters the study area (Fig. 2m), a wide region of anticyclonic (positive) vorticity appears near the box B and near the hurricane center, with a central vorticity exceeding 3.2×10^{-5} s^{-1}. The intensity of the vorticity center is consistent with that of the center of the GLORYS12V1 data in box B (Fig. 2r). After Isaac passes, this central intensity weakens to 1.6×10^{-5} s^{-1}. However, the positive vorticity region does not decrease much (Figs. 2n,o), a result that reflects the ~13-h inertial time scale of the mesoscale ocean's adjustment to forcing. We conclude from these results that additionally assimilating the drifter positions within an eddy-resolving model framework, which provides information at the mesoscale, is more consistent with the reanalysis, and thus we argue more accurate than experiment PROF and FREE.

b. SST and SSH

High-frequency winds with periods less than the ~13-h inertial period induce horizontally polarized inertial gravity waves and oscillations, particularly under the high wind conditions of the eastern sector of the hurricane (Price 1981). As Isaac strengthened to hurricane intensity at 1200 UTC 28 August (Fig. 3), theories of Price (1981) support that these eastern sector surface currents will show a roughly Ekman-like response to the cyclonic winds. Thus, the decrease in SST and lowering of SSH caused by horizontally divergent Ekman pumping is also mainly located along the eastern sector, with a delay of one or two inertial periods following hurricane passage.

We first discuss the results from the eddy-permitting 1/4°-resolution experiments (Figs. 3a,b). By assimilating the drifter positions, the experiment BOTH yields SSTs on the eastern side of the hurricane that are approximately −0.8°C cooler than those of experiment PROF. This strong cooling response suggests that it also has a better representation of surface current divergence and vertical Ekman pumping. At this resolution, however, SSH remains largely unchanged between experiments PROF and BOTH. For example, there is no SSH minimum in the eastern sector of Isaac in either of

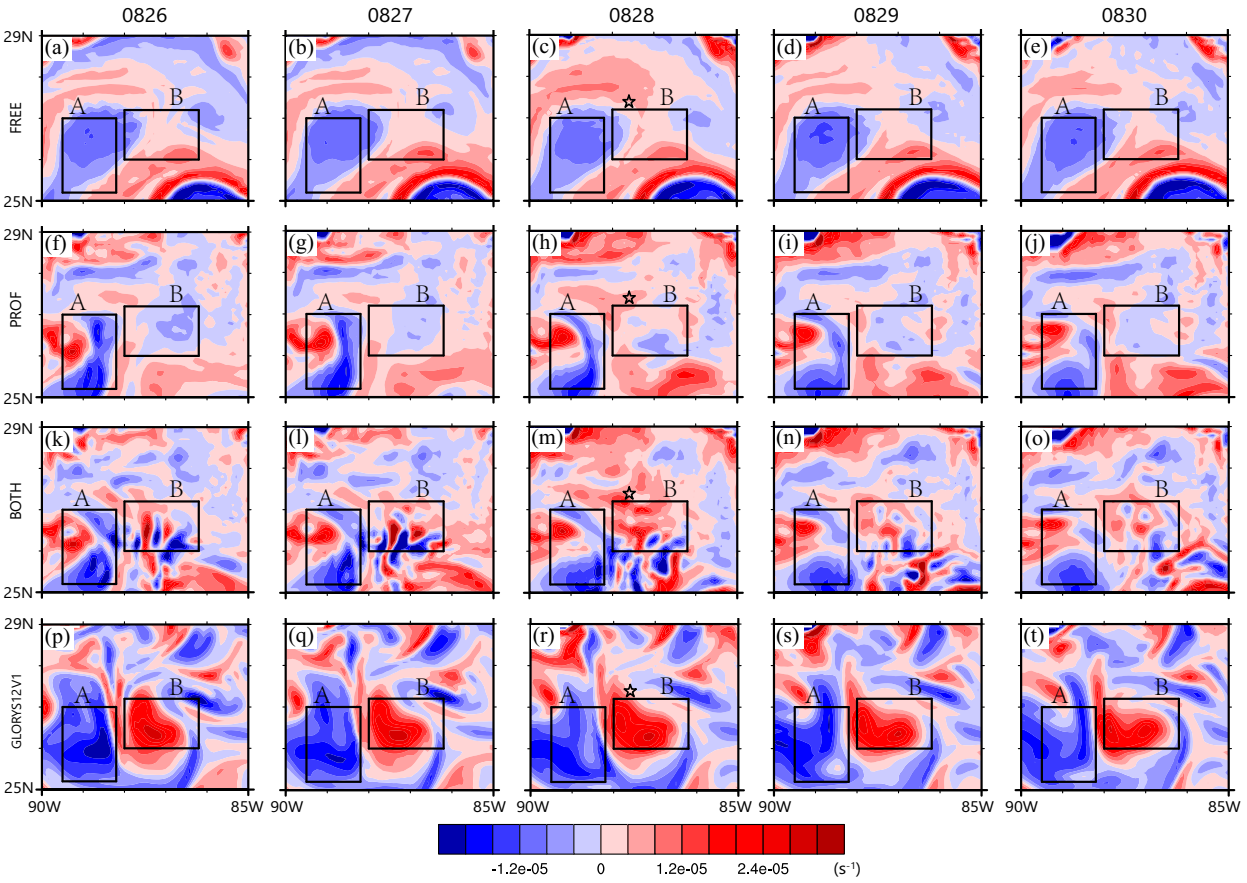

FIG. 2. Daily surface vorticity at 1/12° in the research area (yellow-outlined box in Fig. 1) from 26 to 30 Aug: (a)–(e) experiment "FREE," (f)–(j) experiment PROF, (k)–(o) experiment BOTH, and (p)–(t) GLORYS12V1 reanalysis. Note that the black stars indicate the eye of Hurricane Isaac on 28 Aug, and the black-outlined boxes A and B indicate the locations of the stationary pair of anticyclonic and cyclonic eddies in the GLORYS12V1 reanalysis.

the PROF and BOTH experiments. This lack of impact may be due either to the fact that simulations at this resolution do not incorporate sufficient mesoscale information or to the fact that the intensity of the simulated Ekman pumping is still insufficient to cause a reduction in SSH.

The 1/12° eddy-resolving experiments include much more mesoscale uncertainty than the 1/4° eddy-permitting experiments (Figs. 3c,d). In the previous section, we demonstrated that experiment BOTH exhibits greater consistency with GLORYS12V1 than PROF, particularly in terms of the position and strength of cyclonic eddies. This is also evident in the comparison of positive eddy circulation around point A, as shown in Figs. 3d and 3e. The BOTH SST response to Isaac is markedly asymmetric (Price 1981), with a clear "cold wake" with a central SST of 25.5°C (Fig. 3d, point A) appearing in the eastern sector of the hurricane track. This cooling is the result of horizontal divergence at the sea surface in the vicinity of point A and upwelling of cool subthermocline water. In contrast, horizontal divergence near point B simply upwells warm water from within the deeper thermocline at this location (Fig. 3d) (leaving a "warm wake"). Additionally, the surface currents forced by Isaac west of point B are constantly transporting warm water eastward. This transport slows near point B (a central SST of 32°C), thus causing the warm water to accumulate and the hurricane heat potential to increase. Jourdain et al. (2014) reported that the GLORYS data may underestimate the impact of hurricanes on the upper ocean by up to 30% due to its long data assimilation window of 7 days, resulting in an average underestimation of 50% for the cold wake effect. A comparison of Figs. 3d and 3e shows that experiment BOTH exhibits greater consistency with the instantly actual response of the ocean surface to hurricanes, particularly in terms of SST, than do the GLORYS12V1 reanalysis data where points A and B have similar SST values at 29.5°C.

A difference in SSH is also obvious between the two experiments. A distinct low in SSH (dashed lines) with a central value of −0.08 m in the southeast quadrant is collocated with the cold wake in the experiment BOTH, as expected from the hydrostatic relationship between pressure and density (Fig. 3d). A large range of low SSH matches in the southeast quadrant of GLORYS12V1 (Fig. 3e). However, in the experiment PROF (Fig. 3c), no cold wake appears on the southeast quadrant, and there is no corresponding area of low SSH.

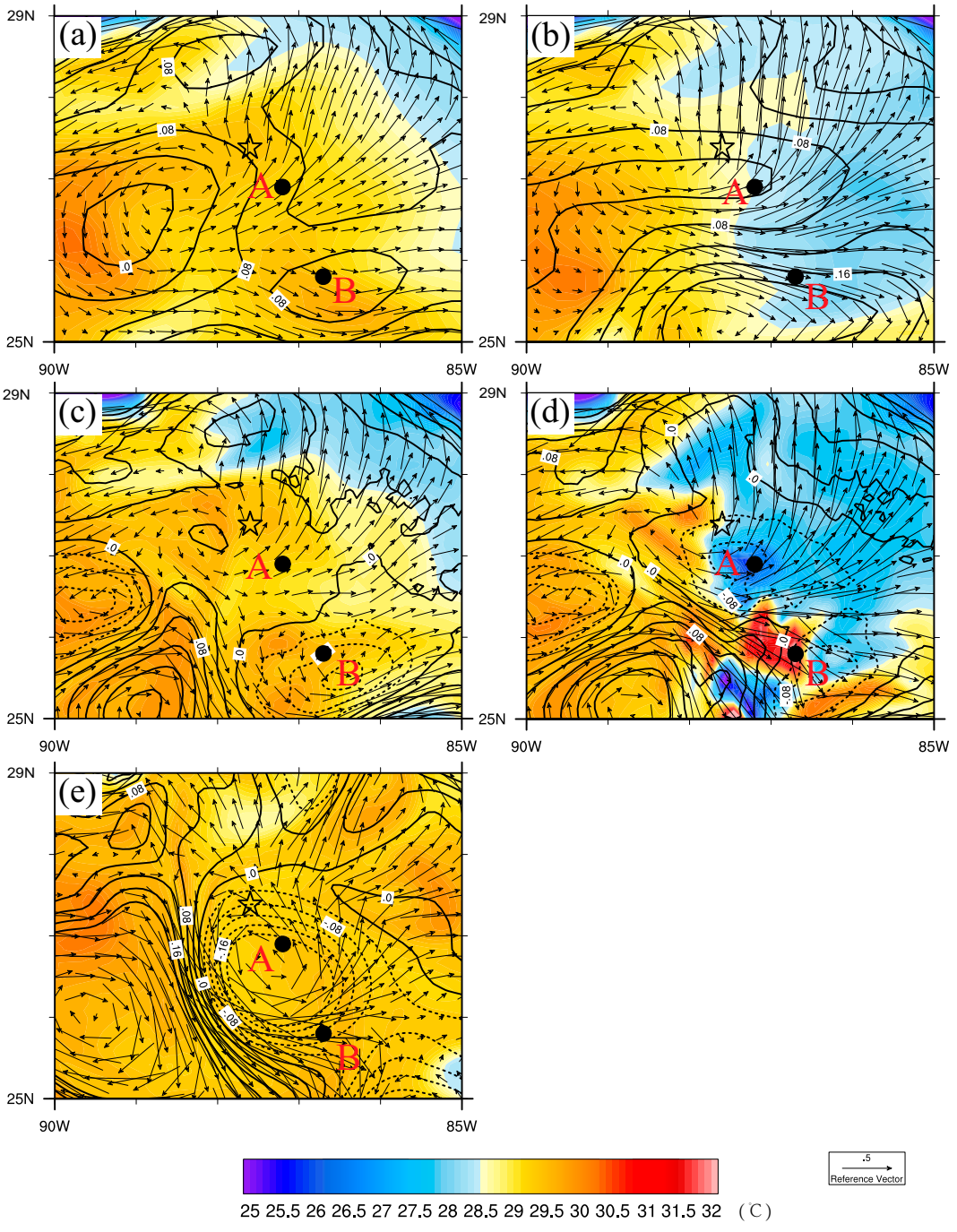

FIG. 3. Comparison of surface ocean variables from different experiments on 28 Aug. Colors show SST, black contours show SSH (m; contour interval is 0.04 m; low values are indicated by the dashed lines), and the vectors indicate the surface current velocity (m s^{-1}). Black stars indicate the eye of Hurricane Isaac, and solid circles A and B indicate the possible locations of cold and warm wakes. (a) Experiment PROF at 1/4° resolution, (b) experiment BOTH at 1/4° resolution, (c) experiment PROF at 1/12° resolution, (d) experiment BOTH at 1/12° resolution, and (e) GLORYS12V1 reanalysis. Note that the area selected in this plot is the yellow-outlined box in Fig. 1.

The reason for the difference in SSH is that experiment BOTH instantly captures the change in surface current caused by Isaac as the result of the LaDA of the drifter positions. Also, the stronger hurricane winds in the eastern sector results in stronger northward-oriented currents. These results are consistent with the surface velocity in the eastern sector in experiment BOTH being stronger than experiment PROF.

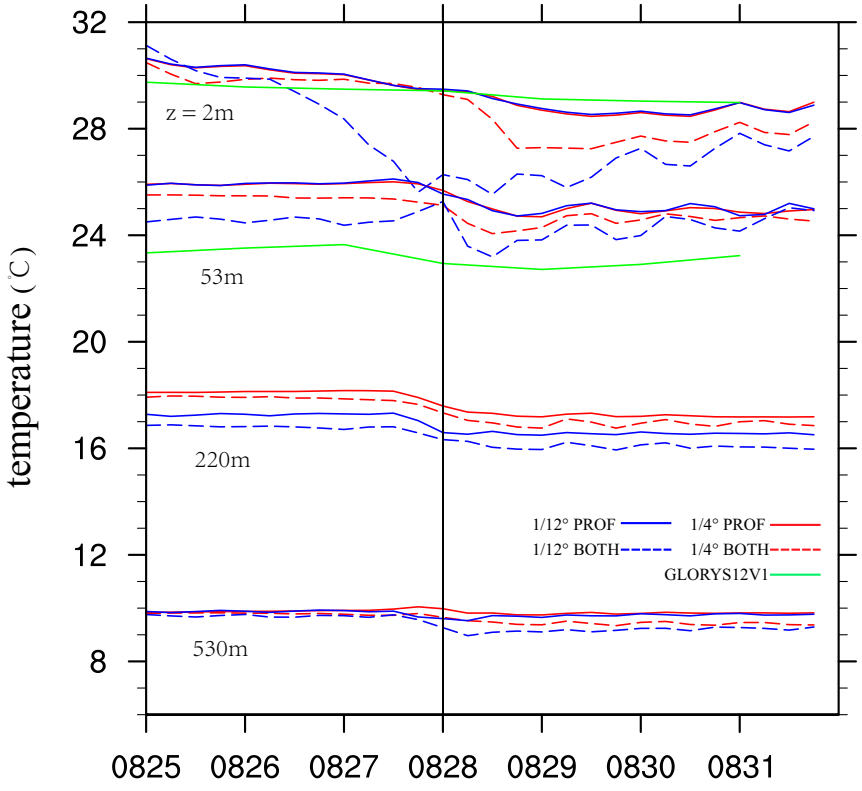

FIG. 4. Change in temperature at different depths at point A (see Fig. 3 for location) with time from 25 to 31 Aug. A vertical line indicates the time of passage of Hurricane Isaac through the research area. For the research focus, the experiments FREE are not presented here and GLORYS12V1 gives reference only in the range of vertical localization (z = 2 and 53 m).

c. *Temperature and salinity*

The BOTH experiment with eddy-resolving 1/12° resolution markedly improves the estimation of the hurricane-induced mixing effect and subsurface temperature change, especially above the OML, when compared with either PROF or BOTH at the eddy-permitting 1/4° resolution. The SST at point A (Fig. 4) of experiment BOTH with 1/12° resolution decreased by an additional −4°C relative to the same resolution of PROF following the passage of Isaac. However, there is no significant difference in temperature between experimental BOTH and PROF at 1/4° resolution at the time of hurricane passage. As previously analyzed, GLORYS12V1 does not reflect the actual impact of hurricanes on SST over time. The mixed layer at point A was initially shallower than 53 m and thus the temperature at this depth was much cooler than SST. Just after the hurricane center passes point A, experiment PROF at eddy-resolving 1/12° resolution has a shallow ~30 m OML (Fig. 5a; Table 1). In contrast, the OML exceeds 53 m in experiment BOTH, suggesting that LaDA of drifter positions can help to capture the impacts of hurricane forcing on mixing and entrainment, which is statistically significant according to the 95% confidence interval in Table 1. At 53 m, GLORYS2V1 reanalysis data always give a temperature that is approximately −1°C than experimental BOTH. In experiment BOTH, temperatures are slightly lower at 220- and 530-m depths (middle and lower thermoclines), indicating that hurricane forcing can also influence temperatures below the thermocline. During the first few days after the hurricane passed in the experiment BOTH, the temperature oscillated with the 53-m temperature with the near-inertial period. The effect of the simulation of the mesoscale response to Isaac on the vertical structure of temperature depends on the resolution (Fig. 4). For example, at point A at 1/4° resolution the temperature dropped by 2°C following the passage of Isaac and the OML remains at ~30-m depth, while at 1/12° the drop was 4°C with a corresponding deepening of the OML. It is noteworthy that thermocline (220–530 m in Fig. 4) cooling remains basically the same at both resolutions.

The impacts on subsurface salinity are shown in Fig. 5b and Table 2. The enhanced entrainment and mixing that occurs at 1/12° resolution produces 100-m salinity rises by ~0.2 psu, whereas the average salinity between 100 and 300 m declines by one-half of that value. In contrast, vertical mixing and entrainment impacts at 1/4° resolution are roughly one-half as large.

4. Discussion and conclusions

This study explored the impact of using the Lagrangian data assimilation technique LETKF-LaDA to assimilate surface drifter path information, particularly focusing on the response

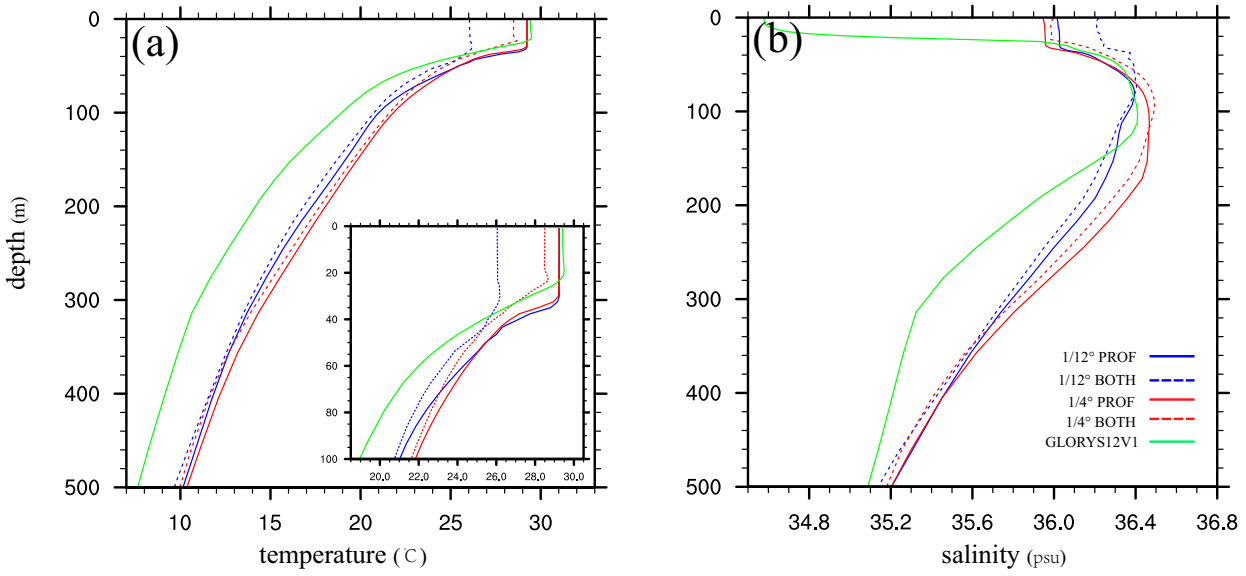

FIG. 5. Vertical profiles of (a) temperature and (b) salinity at point A on 28 Aug (see Fig. 3 for location). The inset plot in (a) focuses on the temperature profile above 100-m depth.

of ocean surface currents and hydrography during the passage of Hurricane Isaac through the Gulf of Mexico in the summer of 2012. Our choice of Hurricane Isaac was guided by the availability of a large set of surface drifters from the GLAD experiment as well as availability of in situ temperature and salinity profile observations. Three types of experiments were carried out: a free run without any updating (FREE), experiments where only hydrographic profiles are assimilated (PROF), and experiments where surface drifter path information is also assimilated (BOTH). Because the results were sensitive to the horizontal resolution of the analysis, we presented experiments using both eddy-permitting 1/4° and eddy-resolving 1/12° model grids. Verification is a challenge for this experiment since there are no independent surface velocity measurements. We used the new GLORYS12V1 reanalysis for evaluation and verification of our experiments.

The results of our study can be summarized as follows:

(i) Assimilation of drifter positions allows for more accurate mesoscale detail of ocean surface current fields, and more accurate changes in the ocean surface current in response to the passage of Hurricane Isaac. Assimilating the drifter positions also improves estimation of the asymmetric (with respect to track) impact of Hurricane Isaac on SST and SSH. For example, assimilating both drifter positions and profiles (BOTH) at 1/4° resolution yielded 0.8 greater decreases in SST than assimilating only profiles (PROF). The BOTH experiment at 1/12° resolution generated a clear eastern sector "cold wake" with a central SST of 25.5°C.

(ii) By analyzing the ocean stratification before and after hurricane passage, we found that assimilating drifter positions impacted the analysis estimate of subsurface temperature and salinity. Assimilating drifter positions cools and deepens the mixed layer while it increases mixed layer salinity due to hurricane-induced mixing/entrainment.

(iii) Improvements due to assimilating surface drifter positions were greater at smaller scales and thus are greater for the 1/12° analysis system. As an example, we showed that SST and SSH had more mesoscale details at 1/12°.

Although this study focused on the Gulf of Mexico, our results highlighting the advantages of LETKF-LaDA combined with a 1/12°-resolution analysis system should be equally applicable to other regions impacted by tropical cyclones, such as the Bay of Bengal. Indeed, we believe the results of this study are sufficiently successful that the proposed method

TABLE 1. The 95% confidence interval of mean temperature (°C) in different levels at point A on 28 Aug for PROF and BOTH experiments in 1/4 and 1/12 systems. Each entry is shown in the form of $A \pm B$, where A is the ensemble mean in the given level and B is the standard error ($B = 1.96s/\sqrt{29}$, with s being the sample standard deviation).

	1/4° PROF	1/4° BOTH	1/12° PROF	1/12° BOTH
1–20 (m)	29.21 ± 0.06	28.34 ± 0.05	29.13 ± 0.06	25.52 ± 0.09
20–40 (m)	28.36 ± 0.11	26.99 ± 0.11	28.42 ± 0.13	25.39 ± 0.10
40–60 (m)	25.83 ± 0.05	24.33 ± 0.04	25.21 ± 0.08	23.48 ± 0.14
60–100 (m)	23.13 ± 0.06	22.62 ± 0.04	22.55 ± 0.08	21.68 ± 0.07

TABLE 2. As in Table 1, but for the salinity (psu).

	1/4° PROF	1/4° BOTH	1/12° PROF	1/12° BOTH
1–20 (m)	35.95 ± 0.02	35.98 ± 0.02	36.01 ± 0.03	35.93 ± 0.03
20–40 (m)	36.02 ± 0.02	36.14 ± 0.01	36.06 ± 0.03	36.04 ± 0.03
40–60 (m)	36.28 ± 0.01	36.38 ± 0.005	36.29 ± 0.01	36.37 ± 0.01
60–100 (m)	36.42 ± 0.005	36.47 ± 0.005	36.39 ± 0.01	36.38 ± 0.01

should be implemented for testing in a coupled operational tropical cyclone forecast system.

Acknowledgments. The authors acknowledge the Monsoon-Mission-II Project entitled "Advancements of the Hybrid Global Ocean System (HYBRID-GODAS) for the Monsoon Mission II (IITM/MM_JI/Univ_Maryland_USA/2018/INT-2/)" for financial support for authors Dong and Sun and for partial support for authors Penny and Carton. Sun was also funded by NOAA Grant NA19NES4320002 (CISESS). Penny acknowledges further support from the Office of Naval Research Grants N00014-19-1-2522 and N00014-20-1-2580.

Data availability statement. Datasets for this research are archived on the Indian Institute of Tropical Meteorology High Performance System Aaditya (http://aadityahpc.tropmet.res.in/Aaditya/index.html) and are available upon request from the authors.

REFERENCES

Berta, M., A. Griffa, M. G. Magaldi, and T. M. Özgökmen, 2015: Improved surface velocity and trajectory estimates in the Gulf of Mexico from blended satellite altimetry and drifter data. *J. Atmos. Oceanic Technol.*, **32**, 1880–1901, https://doi.org/10.1175/JTECH-D-14-00226.1.

Boyer, T. P., O. K. Baranova, C. Coleman, and H. E. Garcia, 2018: *Temperature*. Vol. 4, *World Ocean Database 2018*, NOAA Atlas NESDIS 87, 52 pp.

Cardona, Y., and A. Bracco, 2016: Predictability of mesoscale circulation throughout the water column in the Gulf of Mexico. *Deep-Sea Res. II*, **129**, 332–349, https://doi.org/10.1016/j.dsr2.2014.01.008.

Carton, J. A., G. A. Chepurin, and L. Chen, 2018: SODA3: A new ocean climate reanalysis. *J. Climate*, **31**, 6967–6983, https://doi.org/10.1175/JCLI-D-18-0149.1.

Chelton, D. B., R. A. deSzoeke, M. G. Schlax, and K. El Naggar, 1998: Geographical variability of the first baroclinic Rossby radius of deformation. *J. Phys. Oceanogr.*, **28**, 433–460, https://doi.org/10.1175/1520-0485(1998)028<0433:GVOTFB>2.0.CO;2.

Dee, D. P., S. M. Uppala, A. J. Simmons, and P. Berrisford, 2011: The ERA-Interim reanalysis: Configuration and performance of the data assimilation system. *Quart. J. Roy. Meteor. Soc.*, **137**, 553–597, https://doi.org/10.1002/qj.828.

Elipot, S., and R. Lumpkin, 2008: Spectral description of oceanic near-surface variability. *Geophys. Res. Lett.*, **35**, L05606, https://doi.org/10.1029/2007GL032874.

Hunt, B. R., E. J. Kostelich, and I. Szunyogh, 2007: Efficient data assimilation for spatiotemporal chaos: A local ensemble transform Kalman filter. *Physica D*, **230**, 112–126, https://doi.org/10.1016/j.physd.2006.11.008.

Ide, K., L. Kuznetsov, and C. K. Jone, 2002: Lagrangian data assimilation for point vortex systems. *J. Turbul.*, **3**, 053, https://doi.org/10.1088/1468-5248/3/1/053.

Ishikawa, Y., T. Awaji, K. Akitomo, and B. Qiu, 1996: Successive correction of the mean sea surface height by the simultaneous assimilation of drifting buoy and altimetric data. *J. Phys. Oceanogr.*, **26**, 2381–2397, https://doi.org/10.1175/1520-0485(1996)026<2381:SCOTMS>2.0.CO;2.

Issa, L., J. Brajard, M. Fakhri, D. Hayes, L. Mortier, and P.-M. Poulain, 2016: Modelling surface currents in the eastern Levantine Mediterranean using surface drifters and satellite altimetry. *Ocean Modell.*, **104**, 1–14, https://doi.org/10.1016/j.ocemod.2016.05.006.

Jean-Michel, L., G. Eric, B.-B. Romain, and G. Gilles, 2021: The Copernicus global 1/12° oceanic and sea ice GLORYS12 reanalysis. *Front. Earth Sci.*, **9**, 698876, https://doi.org/10.3389/feart.2021.698876.

Jourdain, N. C., B. Barnier, N. Ferry, J. Vialard, C. E. Menkes, M. Lengaigne, and L. Parent, 2014: Tropical cyclones in two atmospheric (re)analyses and their response in two oceanic reanalyses. *Ocean Modell.*, **73**, 108–122, https://doi.org/10.1016/j.ocemod.2013.10.007.

Kuznetsov, L., K. Ide, and C. K. Jones, 2003: A method for assimilation of Lagrangian data. *Mon. Wea. Rev.*, **131**, 2247–2260, https://doi.org/10.1175/1520-0493(2003)131<2247:AMFAOL>2.0.CO;2.

Lellouche, J.-M., O. Le Galloudec, M. Drévillon, and C. Régnier, 2013: Evaluation of global monitoring and forecasting systems at Mercator Océan. *Ocean Sci.*, **9**, 57–81, https://doi.org/10.5194/os-9-57-2013.

——, and Coauthors, 2021: The Copernicus global 1/12° oceanic and sea ice reanalysis. *EGU General Assembly 2021*, online, Copernicus Meetings, EGU21-14961, https://doi.org/10.5194/egusphere-egu21-14961.

Lumpkin, R., T. Özgökmen, and L. Centurioni, 2017: Advances in the application of surface drifters. *Annu. Rev. Mar. Sci.*, **9**, 59–81, https://doi.org/10.1146/annurev-marine-010816-060641

Madec, G., and the NEMO Team, 2008: NEMO ocean engine. Note du Pôle de Modélisation de l'Institut Pierre-Simon Laplace 27, 300 pp.

Molcard, A., L. I. Piterbarg, A. Griffa, T. M. Özgökmen, and A. J. Mariano, 2003: Assimilation of drifter observations for the reconstruction of the Eulerian circulation field. *J. Geophys. Res.*, **108**, 3056, https://doi.org/10.1029/2001JC001240.

Muscarella, P., M. J. Carrier, H. Ngodock, S. Smith, B. L. Lipphardt, A. D. Kirwan, and H. S. Huntley, 2015: Do assimilated drifter velocities improve Lagrangian predictability in an operational ocean model? *Mon. Wea. Rev.*, **143**, 1822–1832, https://doi.org/10.1175/MWR-D-14-00164.1.

Nilsson, J. A., S. Dobricic, N. Pinardi, P.-M. Poulain, and D. Pettenuzzo, 2012: Variational assimilation of Lagrangian

trajectories in the Mediterranean Ocean Forecasting System. *Ocean Sci.*, **8**, 249–259, https://doi.org/10.5194/os-8-249-2012.

NOAA–GFDL, 2021: Welcome to MOM6's documentation. Accessed 12 May 2021, https://mom6.readthedocs.io/en/dev-gfdl/.

Nodet, M., 2006: Variational assimilation of Lagrangian data in oceanography. *Inverse Probl.*, **22**, 245–263, https://doi.org/10.1088/0266-5611/22/1/014.

Özgökmen, T., 2012: GLAD experiment CODE-style drifter trajectories (low-pass filtered, 15 minute interval records), northern Gulf of Mexico near DeSoto Canyon, July–October 2012. Gulf of Mexico Research Initiative Information and Data Cooperative (GRIIDC), Harte Research Institute, Texas A&M University–Corpus Christi, accessed 7 April 2022, https://doi.org/10.7266/N7VD6WC8.

Penny, S. G., D. W. Behringer, J. A. Carton, and E. Kalnay, 2015: A hybrid global ocean data assimilation system at NCEP. *Mon. Wea. Rev.*, **143**, 4660–4677, https://doi.org/10.1175/MWR-D-14-00376.1.

Price, J. F., 1981: Upper ocean response to a hurricane. *J. Phys. Oceanogr.*, **11**, 153–175, https://doi.org/10.1175/1520-0485(1981)011<0153:UORTAH>2.0.CO;2.

Slivinski, L. C., G. P. Compo, J. S. Whitaker, and P. D. Sardeshmukh, 2019: Towards a more reliable historical reanalysis: Improvements for version 3 of the twentieth century reanalysis system. *Quart. J. Roy. Meteor. Soc.*, **145**, 2876–2908, https://doi.org/10.1002/qj.3598.

Sluka, T. C., S. G. Penny, E. Kalnay, and T. Miyoshi, 2016: Assimilating atmospheric observations into the ocean using strongly coupled ensemble data assimilation. *Geophys. Res. Lett.*, **43**, 752–759, https://doi.org/10.1002/2015GL067238.

Sun, L., and S. G. Penny, 2019: Lagrangian data assimilation of surface drifters in a double-gyre ocean model using the local ensemble transform Kalman filter. *Mon. Wea. Rev.*, **147**, 4533–4551, https://doi.org/10.1175/MWR-D-18-0406.1.

——, ——, and M. Harrison, 2022: Impacts of the Lagrangian data assimilation of surface drifters on estimating ocean circulation during the Gulf of Mexico grand Lagrangian deployment. *Mon. Wea. Rev.*, **150**, 949–965, https://doi.org/10.1175/MWR-D-21-0123.1.

Taillandier, V., and A. Griffa, 2006: Implementation of position assimilation for ARGO floats in a realistic Mediterranean Sea OPA model and twin experiment testing. *Ocean Sci.*, **2**, 223–236, https://doi.org/10.5194/os-2-223-2006

Trent, K. R., 2006: Effect of the Gulf of Mexico's mixed layer depth on hurricane intensity in the warming environment. SOARS Protégé Research Papers Summer 2006, University Corporation for Atmospheric Research, 26 pp., https://doi.org/10.5065/zf2q-1956.

Vernieres, G., C. K. R. T. Jones, and K. Ide, 2011: Capturing eddy shedding in the Gulf of Mexico from Lagrangian observations. *Physica D*, **240**, 166–179, https://doi.org/10.1016/j.physd.2010.06.008.